Title: Food entrainment in mice leads to sex- and organ-specific responses in the digestive system and nutrient metabolism

Short title: Food intake as a zeitgeber in the murine digestive system

Lalita Oparija-Rogenmozere[1,2,5,$], Madeleine R. Di Natale[1,2,$], Billie Hunne[1], Ada Koo[1], Mitchell Ringuet[1], Therese E. Fazio Coles[1], Linda J. Fothergill[1], Rachel McQuade[3,4,#,*], John B. Furness[1,2,#]

[1]Department of Anatomy and Physiology, The University of Melbourne, Parkville, Victoria 3052, Australia

[2]The Florey Institute of Neuroscience and Mental Health, Parkville, Victoria 3052, Australia

[3]Gut Barrier and Disease Laboratory, Department of Anatomy & Physiology, The University of Melbourne, Parkville, VIC 3010, Australia

[4]Australian Institute for Musculoskeletal Science (AIMSS), Western Centre for Health Research and Education (WCHRE), Sunshine Hospital, St Albans, VIC 3021, Australia

[5]Current affiliation: Department of Biomedicine, University of Basel, 4058 Basel, Switzerland

[$]Equal first authors

[#]Equal last authors

*Corresponding author. Mailing address: Dr. Rachel McQuade, Gut Barrier and Disease Laboratory, Department of Anatomy & Physiology, The University of Melbourne. Parkville, VIC 3010, Australia. Phone: +61 3 9035 5511, E-mail: rachel.mcquade@unimelb.edu.au.

Abstract

One of the main zeitgebers in the digestive system is food intake; however, little is known about organ- and sex-specific differences in food-driven circadian regulation. We placed male and female C57Bl/6 mice on time-restricted feeding (TRF), limiting food intake period to 8 hours. TRF was started either at dark (ZT12) or light (ZT0) onset and continued for 28 days, with or without an additional 4 hour forward shift on day 15.

TRF from ZT12 to ZT20 led to the highest weight gain in females, but the lowest weight gain in males, while improving intestinal transepithelial resistance (TEER) in both sexes. Unexpectedly, it also led to the disappearance of diurnal rhythmicity in several hepatic genes. Shifting the TRF start to ZT16 led to an increase in weight gain and a decrease in fasting plasma glucose levels in male mice, as well as to strong rhythmicity in nutrient metabolism-related hepatic and duodenal genes in both sexes. Surprisingly, food intake during ZT0-ZT8 caused only minor changes in physiological responses. However, it did lead to an overall downregulation of gene expression in the liver, an upregulation in the stomach and duodenum, and to flattened diurnal responses. Shifting the start of food intake to ZT4 was highly detrimental, causing an increase in fasting blood glucose levels, a decrease in TEER, and disrupting diurnal gene expression pattern in the

liver and stomach. Despite this, in duodenum TRF from ZT4 to ZT12 acted as a potent zeitgeber.

These results demonstrate that the adjustment to food intake time in mice is highly sex- and organ-specific. Our chosen TRF regimes were not able to achieve full diurnal rhythm synchronization across the digestive system. Instead, we observed that the same food intake time might be a strong zeitgeber in one organ, and a rhythm disruptor in another.

Keywords

Diurnal, digestive system, digestive clocks, sex-specific differences, food intake time, peripheral zeitgebers, nutrient metabolism

Introduction

Our daily schedule and meal times cause rhythmic variations in environmental and nutritional stimuli, leading to the generation of circadian rhythms to help our body anticipate recurring events (Albrecht, 2012). Early work on the existence of circadian rhythms in mammals revealed diurnal oscillations in body temperature (Kleitman and Engelman, 1947; Rodbard, 1947; Mellette et al., 1951), food intake (Goetzl and Stone, 1947) and specific organ functions, e.g., rhythmic renal excretion of water and salts (Sirota and Baldwin, 1950; Mills, 1951). In humans the circadian period is approximately 24h long and seems to be influenced by age, race, geographical location, and, possibly, sex (Mills, 1964; Forni et al., 2014; Eastman et al., 2016; Crowley and Eastman, 2018). It has been observed that humans placed in an environment without any indication of the time of day, can preserve their previous circadian activity rhythm (Crawford and Thor, 1964), indicating certain rhythm stability. In 1945 the term “zeitgeber” (time-giver) was introduced to describe stimuli that affect the timing of the daily rhythm of any biological process within an organism (Aschoff, 1945). At present, the daily light-dark cycle is the best researched zeitgeber; other known zeitgebers include food (content and intake time), temperature, exercise, and drugs of abuse (Schibler et al., 2015; Lewis et al., 2018; Gillman et al., 2019; Begemann et al., 2020).

Simplistically, the mammalian molecular circadian clock is a transcriptional feedback loop, expressed in almost every cell, driving expression patterns of multiple core clock genes with approximately 24-hour rhythmicity. The positive limb of this feedback loop consists of two master transcription factors: CLOCK (circadian locomotor output cycles kaput) and BMAL1 (brain and muscle ARNT-like protein), which form a heterodimer. The CLOCK-BMAL1 heterodimer binds to the promoters of its target genes, including those comprising the negative limb of the feedback loop: *Per1*, *Per2*, *Per3* (further: PERs – mammalian analogues of the *Drosophila period* gene) and *Cry1*, *Cry2* (further: CRYs). PERs and CRYs then dimerize, translocate back to the nucleus, and inhibit the activity of CLOCK-BMAL1 heterodimer, subsequently inhibiting their own expression (for extensive reviews on core clock function and mechanism see: (Albrecht, 2012; Takahashi and Lowrey, 2000; Buhr and Takahashi, 2013; Buijs et al., 2016; Hastings et al., 2018; Cox and Takahashi, 2019)). There are also multiple secondary loops modulating the output of the core clock, such as the orphan nuclear receptor families REV-ERBs and RORs. Both of these families have been suggested to provide a link between metabolism and the circadian clock, especially towards the regulation of lipid metabolism (Duez and Staels, 2008; Solt et al., 2011). In addition to the translational regulation, the circadian clock is also regulated post-translationally, with multiple kinases, phosphatases, microRNAs and RNA-

binding protein complexes modulating various aspects and the output of the core clock (Albrecht, 2012).

A central circadian oscillator is located in the suprachiasmatic nucleus (SCN) of the hypothalamus, receiving inputs from environmental signals (e.g., light) and conveying the generated rhythms to the periphery both directly via neural and hormonal signalling and indirectly via regulation of body temperature. However, peripheral tissues such as the gastrointestinal (further: GI) tract and liver also possess self-sustaining, entrainable circadian rhythms, with food entrainment being the most potent zeitgeber (Damiola et al., 2000; Welsh et al., 2010). It has been shown that peripheral zeitgebers are even able to override the central, light-entrained rhythms (Damiola et al., 2000; Balakrishnan et al., 2010); however, the overall knowledge of peripheral clock entrainment is fragmented as research has been skewed towards specific organs. The food-entrained circadian clock has been extensively studied in the liver, but somewhat neglected in the digestive system, despite the gut being vital for food intake, breakdown, and absorption. To investigate the role of food intake in circadian rhythm generation, time-restricted feeding (further: TRF) is commonly used over prolonged periods of time, as it has been shown that food intake after a long fast (≥12 h) is a strong determinant of the peripheral clock phase (Kuroda et al., 2012).

Another poorly investigated area is sex-specific circadian rhythms. Research in rodents has shown that the morphology and neuropeptide expression in SCN differ between males and females. Human studies have mostly focused on sex differences in sleep rhythms, showing that women exhibit an earlier sleep phase and a longer circadian period. Both rodent and human studies have also shown sex differences in corticosteroid secretion (for reviews on sex differences see (Yan and Silver, 2016; Silver, 2018)). When it comes to the food entrainment, male mice have been shown to develop an earlier and higher-amplitude food-anticipatory behaviour when compared to female mice (Aguayo et al., 2018). Despite this evidence of sex-specific differences in circadian rhythmicity, they have been poorly studied at the molecular level, especially regarding nutrient handling and metabolism.

As circadian rhythms coordinate physiological responses depending on the anticipated stimuli, they can be disturbed when these stimuli are changed, e.g., by changes in caloric intake, during shift work, travel between time zones, or eating during the resting phase. Disruption of the clock has been shown to play such a major role in the development and comorbidities of metabolic syndrome and obesity, that there exists a suggestion to rename the metabolic syndrome “circadian syndrome” (Zimmet et al., 2019). Consequently, synchronization of diurnal rhythms seems to lead to the opposite effect: TRF in coordination with the

body's daily rhythm has beneficial effects on general health (Asher and Sassone-Corsi, 2015; Voigt et al., 2019), although organ-specific responses to particular feeding rhythms have not been studied in detail.

To investigate clock-dependent, sex-specific regulation of nutrient metabolism in the digestive system, we placed male and female mice on 8 h TRF starting either at the onset of dark or light phase. Our investigation focused on weight gain, fasting glucose values, intestinal transepithelial resistance (further: TEER) and clock- and metabolism-related gene expression. In addition, we investigated the effects of a 4 h food intake time shift within the same light-dark cycle period.

Materials and Methods

Ethical approval

All experimental procedures and handling involving mice were approved by the University of Melbourne Animal Ethics Committee (application #1914983) and performed in compliance with the Australian code for the care and use of animals for scientific purposes.

Experimental animal origin and housing

In total 180 male and 180 female C57Bl/6 mice (RRID:IMSR_JAX:000664) from Animal Resources Centre (Canning Vale, WA, Australia) were used in the study. All mice arrived to the local animal facility aged 5-7 weeks and were kept under a 12:12 h light-dark (further: LD) cycle, with standard chow (Barastoc 102108, Ridley Corporation, Melbourne, Australia) and water provided *ad libitum*. After three days of post-arrival adjustment to the local facility, mice were transferred to either LEDDY cages (black cages with individual lighting systems) (Cat# GM500) or to the Aria ventilated cabinet (Cat# 9BIOC44R4Y1, both from Tecniplast, Buguggiate, Italy), and the light onset of 12:12 h LD cycle was adjusted such that the sample collection from day-fed and night-fed mice could be done in parallel. Mice were adjusted to the new 12:12 h LD cycle and housing conditions for 1 week, with chow and water provided *ad libitum*. All mice were weighed at the end

of the dark phase (Zeitgeber time (ZT) 24). Obtained values were recorded as pre-time-restricted feeding weights (further: pre-TRF) and used as a baseline for later weight gain calculations.

Food-entrainment of mice

After a 1-week adjustment to the new LD cycle, mice were subjected to TRF for 14 days (Fig. 1, Pre-shift days) «Insert Fig.1». During this time, mice were fed standard chow for 8 h starting either from the dark onset at ZT12 (Fig. 1, Restricted night-fed, grey bar) or the light onset at ZT0 (Fig. 1, Restricted day-fed, yellow bar), followed by a 16 h fasting period. To ensure that mice did not feed on chow debris during fasting, TRF was done by using two cages: a chow-containing cage ("food cage") and a cage that never contained any chow ("empty cage"). Mice were placed in the "food cage" during the feeding period and in the "empty cage" during the fasting period. Water was always provided *ad libitum* for the whole duration of the experiment. Mice were weighed weekly, at the end of their respective feeding period (Fig. 1, blue arrows).

After 14 days of the initial entrainment, for half of the mice the 8 h feeding period was shifted 4 h forward (Fig. 1, Day 15). The new feeding groups were labelled as 'Restricted shifted night-fed' (Fig. 1, ZT16-ZT0, dark grey bar) and 'Restricted shifted day-fed' (Fig. 1, ZT4-ZT12, orange bar). The other half of the mice continued with their initial feeding regimen. Weekly weight gain measurements

were continued as previously stated (Fig. 1, blue arrows,). On the 3rd, 7th and 14th day after the shift, mice were sacrificed for organ collection. Three timepoints were chosen to assess food-driven diurnal responses on each sacrifice day: 1) food anticipation: after 16 h of fasting, right before the anticipated transfer to “food cage” (Fig. 1, “A”); 2) food intake: 4 h after the mice were placed in the “food cage” (Fig. 1, “F”); 3) postprandial period: 4 h after the mice were placed in the “empty cage” (Fig. 1, “P”). On each sacrifice day n=5 female and n=5 male mice were sacrificed at each timepoint.

Mice were anaesthetised with isoflurane (Cat# FGISO0250, Pharmachem, Eagle Farm, Australia) followed by a cervical dislocation. Upon sacrifice, their body weight was measured, and the following organs and tissues were collected and snap frozen using liquid nitrogen: the right lobe of the liver, the dorsal half of the stomach and the duodenal mucosa. To collect duodenal mucosa, the first 2 cm of duodenum were opened and scraped with a surgical scalpel at 45° angle. Ileum (5 cm proximal from the cecum) was collected only during the food intake timepoint (Fig. 1, “F”), and used to measure intestinal permeability and transepithelial electrical resistance.

Blood glucose measurements

Blood glucose was measured at the food anticipation timepoint, after 16 h fasting (Fig. 1, “A”). A drop of blood from tail vein was applied on Accu-Chek® Performa

Test strip (Cat# 06454038020) and glucose concentration was measured with Accu-Chek® Performa (Cat# 05894964014) blood glucose meter (both from Roche Diagnostics, Manheim, Germany).

Intestinal electrical resistance measurements

Ileum collected during the food intake timepoint (Fig. 1, “F”) was cut in half. Both pieces were placed in Krebs-Henseleit buffer (11.1 mM glucose, 118 mM NaCl, 4.8 mM KCl, 1.0 mM NaH_2PO_4, 1.2 mM $MgSO_4$, 25 mM $NaHCO_3$, 2.5 mM $CaCl_2$, pH 7.4), opened along the mesenteric border and pinned (full-thickness) onto Ussing chamber sliders (Cat# P2311, 0.3 cm^2 apertures, Physiological Instruments, San Diego, USA). Sliders were inserted in the middle of two-part Ussing chambers (EasyMount Diffusion Chambers, Physiologic Instruments, San Diego, USA) and 5 ml Krebs-Henseleit buffer solution was added to the serosal side of the tissue. The mucosal side of the tissue received 5 ml of modified Krebs-Henseleit buffer where glucose was substituted with 11.1 mM mannitol. This was done to avoid apical uptake of glucose while still maintaining an osmotic balance. Buffers in both chambers were kept at 37°C and bubbled with carbogen (5% CO_2, 95% O_2) to maintain an optimal pH level. A multichannel voltage-current clamp (VCC MC6, Physiologic Instruments, San Diego, USA) was applied to each chamber through a set of four electrodes (2 voltage sensing and 2 current passing electrodes) and agar bridges (3% agarose/3 M KCl in the tip and backfilled with

3 M KCl), installed on opposite sides of the tissue. The tissue was left to equilibrate for 20 min before clamping the voltage to 0 V.

To calculate TEER ($\Omega \cdot cm^2$), 2 sec pulses of 2 mV were administered to tissue every 60 sec for 1 h, and the measured net resistance was multiplied by the surface area. Voltage and short circuit current (Isc) measurements were recorded using a PowerLab amplifier and the software LabChart® 5 (RRID:SCR_017551, both ADInstruments, Sydney, Australia).

RNA extraction

Total RNA from approx. 20 mg of the right lobe of the liver, dorsal half of the stomach and scraped duodenal mucosa was extracted using ISOLATE II RNA Mini Kit (Cat# BIO-52073, Meridian Bioscience, Cincinnati, USA) with the following adjustments to the manufacturer's instructions. First, tissue pieces were immediately snap frozen in 2 ml screw cap tubes containing Lysing Matrix D (Cat# 6540-434, Lot# 99999, MP Biomedicals, Irvine, USA) and stored at -80°C until further processing. Second, the volume of provided lysis buffer was increased to 500 µl per sample, and 5 µl of β-mercaptoethanol was added. Lysis buffer was applied while the samples were still frozen and immediately followed by lysis at 6000 rpm for 2 x 30 sec in a Precellys 24 homogenizer (RRID:SCR_022979, Cat# 03119-200-RD010, Bertin Technologies SAS, Montigny-le-Bretonneux, France). The volume of RNAse free Ethanol (Cat# EA043, Chem-supply, Gillman,

Australia), used for RNA binding, was also increased to 500 µl per sample and lysate-Ethanol filtration through the provided column was done in two consecutive steps. The centrifugation time for all washing steps was increased to 1 min, to ensure better removal of wash buffers. Samples were eluted in 100 µl (liver) or 60 µl (stomach, duodenal mucosa) of RNase free water (Cat# 10977-015, Lot# 2186758, Invitrogen by Life Technologies, Grand Island, USA). The elution step was repeated using the initial eluate to increase the RNA yield. The quality and quantity of the extracted RNA were assessed using 2200 Tape Station (RRID:SCR_014994, Agilent Technologies, Santa Clara, USA) and a Nanodrop ND-1000 UV spectrophotometer (RRID:SCR_016517, NanoDrop Technologies, Wilmington, USA), respectively. The isolation was randomized and done in small batches (24 samples), to ensure fast processing and good RNA quality.

The synthesis of cDNA was performed using 100 ng RNA in a 20 µl total reaction volume using iScript Reverse Transcription Supermix kit (Cat# 1708841, Bio-Rad, Hercules, USA), without any changes from the manufacturer's instructions. Samples were split across 96-well plates, with 6 negative controls (-RT) included on each plate, these were randomly chosen RNA samples where no cDNA synthesizing enzyme was added. Synthesis reaction was carried out using PCRExpress (Cat# 630-003, Thermo Hybaid, Franklin, USA) or Bio-Rad T100™ (RRID:SCR_021921, Bio-Rad, Hercules, USA) thermal cyclers.

Determination of gene expression

After cDNA synthesis, 10 µl of each cDNA sample were delivered to the Translational Research Facility within Monash Health Translational Precinct to determine gene expression levels using the Fluidigm Digital Array Integrated Fluidic Circuits (Ramakrishnan et al., 2013) (further: IFCs). First, all cDNA samples underwent quality control, where expression of either *Gapdh* (forward primer: TGACCTCAACTACATGGTCTACA, reverse: CTTCCCATTCTCGGCCTTG) or *β-actin* (forward primer: GGCTGTATTCCCCTCCATCG, reverse: CCAGTTGGTAACAATGCCATGT) was tested as SYBR assays using QuantStudio 6 Flex RealTime PCR reader (RRID:SCR_020239, Thermo Fisher Scientific, Waltham, USA). Afterwards, samples underwent pre-amplification according to the manufacturer's instructions (Fluidigm, 2015). In short, all 24 TaqMan assays for genes of interest (Table 1) were first pooled and diluted in Tris-EDTA buffer (pH 8.0) to a final concentration of 180 nM per assay. Then 3.75 µl of gene assay mix was added to 1.25 µl of cDNA sample and pre-amplified for 14 cycles using Veriti™ 96-well Thermal Cycler (RRID:SCR_021097, Cat# 9902, Thermo Fisher Scientific, Waltham, USA). Pre-amplified cDNA samples were further diluted 1:5 with Tris-EDTA buffer (pH 8.0) and loaded on the 192.24 Dynamic array IFC (Cat#100-6266, multiple lots used, Fluidigm, San Francisco, USA) together with gene assays, in

accordance with Fluidigm® 192.24 Real-Time PCR Workflow Quick Reference PN 100-6170 (Fluidigm, 2015). The qPCR reaction was performed using Biomark™ HD system (RRID:SCR_022658, Cat# BMKHD, Fluidigm, San Francisco, USA).

Table 1. TaqMan Gene assays used to determine relative gene expression levels

Assigned group by function	**Gene**	**Gene accession number**	**Assay ID**	**Tested in samples from:**
Reference gene	*18s (Rn18s)*	NR_003278.3	Mm04277571_s1	Liver, stomach, duodenum
Core clock genes	*Clock*	NM_001289826.1	Mm00455950_m1	
	Bmal1 (Arntl)	NM_001243048.1	Mm00500226_m1	
Glucose sensing, transport and metabolism	*Tas1r2*	NM_031873.1	Mm00499716_m1	
	Sglt1 (Slc5a1)	NM_019810.4	Mm00451203_m1	
	Glut2 (Slc2a2)	NM_031197.2	Mm00446229_m1	
	Pepck (Pck1)	NM_011044.2	Mm01247058_m1	
	Gys2	NM_145572.2	Mm01267381_g1	Liver
Amino acid and peptide transport	*Pept1 (Slc15a1)*	NM_053079.2	Mm04209483_m1	Liver, stomach, duodenum
	B^0at1 (Slc6a19)	NM_028878.3	Mm01352157_m1	
Lipid metabolism	*Mttp*	NM_001163457.1	Mm00435015_m1	
	Fasn	NM_007988.3	Mm00662319_m1	
	Cyp7a1	NM_007824.2	Mm00484152_m1	
	Pparα	NM_001113418.1	Mm00440939_m1	
	Srebf1	NM_011480.3	Mm00550338_m1	Liver

Biosynthesis of NAD+	*Nampt*	NM_021524.2	Mm00451938_m1	
Hormone signalling	*Ffg21*	NM_020013.4	Mm00840165_g1	
	Igf-1	NM_001111274.1	Mm00439560_m1	
	Tph1	NM_001136084.2	Mm01202614_m1	Stomach and duodenum
	Sst	NM_009215.1	Mm00436671_m1	
	Ghrl	NM_001286404.1	Mm00612524_m1	
	Gast	NM_010257.3	Mm00439059_g1	Stomach
	Lepr	NM_001122899.1	Mm00440181_m1	
	Pga5	NM_021453.4	Mm01208256_m1	
	Gip	NM_008119.2	Mm00433601_m1	Duodenum
	Gcg	AF276754.1	Mm00801714_m1	
	Cck	NM_031161.4	Mm00446170_m1	
Pro-/Anti-inflammatory response	*TNFα*	NM_013693.3	Mm99999068_m1	Liver, stomach, duodenum
	Il-6	NM_031168.1	Mm00446190_m1	
	Il-17a	NM_010552.3	Mm00439619_m1	
	Crp	NM_007768.4	Mm00432680_g1	Liver
	Gpx1	NM_008160.6	Mm00656767_g1	
	Gpx2	NM_030677.2	Mm00850074_g1	Stomach and duodenum

18s was used as a reference gene for the calculation of relative expression ratios (R), using the following formula: $R = 2^{-(Ct(test\ RNA)-Ct(18S\ RNA))}$. All relative expression ratios were further normalized against the average value shown by night-fed males at food anticipation timepoint (Fig. 1, point “A”), on the 3rd day after the feeding shift. All gene expression data and calculated values have been provided as Supplementary datasets (S1-3).

Data analysis and statistics

Experimental data analysis was performed using GraphPad Prism v8.2 (RRID:SCR_002798, GraphPad software, San Diego, CA, USA). To demonstrate weight gain (Fig. 2A), data from each individual mouse within the same feeding group and sex (n=90 for pre-TRF, week 1 and week 2; n = 30 for week 3, n = 15 for week 4) were pooled and shown as a mean group value and 95% Confidence Interval, CI. Differences in weight gain between the night-fed group (= controls) and other feeding groups were assessed by Two-way analysis of variance (ANOVA) with Šidák's multiple comparison test.

Measured TEER values were submitted to an outlier test, with all values outside of mean +/- 2*standard deviation interval excluded from further analysis. This was done to exclude tissue pieces that might have been damaged during the resistance measurements.

Weight at the time of sacrifice (Fig. 2B), fasting blood glucose values (Fig. 2C), and TEER values (Fig. 2D) were shown as separate data points per individual mouse, together with the mean group value and standard deviation (Further: SD) indicated as lines. Two-way ANOVA was used together with Dunnett's multiple comparison test to show differences between feeding groups (night-fed as a control) and sacrifice days (Day 3 post-shift as a control).

To show gene expression differences across timepoints and feeding conditions normalized relative expression ratios representing the same feeding group, sacrifice timepoint and sex were pooled together and shown as a tile within a heatmap. Fold changes in gene expression were shown as Log2 values. The nonparametric Kruskal-Wallis test together with Dunn's multiple comparison test was used to assess the diurnal differences in gene expression (=diurnal change), using the food anticipation group as a control (Figs. 3-6). The p-values were shown as: $^{*}p \leq 0.05$, $^{**}p \leq 0.01$, $^{***}p \leq 0.001$, $^{***}p \leq 0.0001$. Differences in gene expression introduced by the 4 h feeding shift (=baseline change) were assessed with the same statistical test, comparing values between shifted and non-shifted groups at the same timepoint (e.g., night-fed postprandial vs. shifted night-fed postprandial) (Figs. 3-6). The p-values were shown as: $^{£}p \leq 0.05$, $^{££}p \leq 0.01$, $^{£££}p \leq 0.001$, $^{££££}p \leq 0.0001$.

Results

Effects of food entrainment on weight gain, fasting plasma glucose levels and intestinal permeability

Weight gain shows a sex-specific response to food entrainment

Baseline weights (Fig. 1, small arrows) were recorded one day before mice were placed on time-restricted feeding (pre-TRF). All mice started TRF (further: TRF) as either day-fed (further: DF) or night-fed (further: NF) and remained on this regime for 2 weeks. Half of the mice then underwent an additional 4 h forward feeding shift, creating shifted night-fed (further: SNF) and shifted day-fed (further: SDF) groups. The other half of the mice remained on their initial TRF regime. Weight gain was assessed weekly, at the end of the respective feeding periods. Afterwards, all experimental weights were related to the individual pre-TRF values and expressed as a change in percentage (%) over time. Weight gain in NF group was used as a control value, since this feeding regimen is the closest to the natural food intake pattern in mice (Xie et al., 2020).

We observed striking sex-specific differences in weight gain between the feeding groups. At the end of the 2nd entrainment week, DF males showed a significant, 2.9% increase in weight, when compared to their night-fed counterparts (Fig. 2A, in yellow vs. in grey) «Insert Fig.2». No such differences were initially seen in

female mice; however, by the end of the 3rd week of food-entrainment, DF and SDF female mice started showing a significant delay in weight gain when compared to the NF group (-4.4% and -4.7%, respectively) (Fig. 2A in yellow and orange vs. grey). This delay seemed to partially resolve by the end of the 4th entrainment week, with only SDF mice still showing significantly slowed (-4.3%) weight gain. No differences in weight gain were observed between NF and SNF females. These results suggest that in female mice the food intake during the lights-on phase could be detrimental to weight gain. The opposite was seen in male mice. Under longer entrainment, the initially increased weight gain in DF male mice seemed to plateau and was no longer different from NF controls by the end of the experiment (Fig. 2A, yellow vs. grey). At the same time, both 4 h feeding shifts led to an approximately 2.8% increase in weight gain by the end of week 3 (Fig. 2A, in black and orange vs. grey). This response was sustained in SDF mice, leading to a significant, 3.9% weight gain increase by the end of week 4 (Fig. 2A, orange vs. grey).

Overall, day feeding led to an early increase in weight gain in males, and to a delayed weight gain in females over time. In addition, the weight gain in male mice seemed to be more sensitive to the 4 h feeding shift than in females, demonstrating sex-specific weight gain adaptation to the food intake time.

Female mice fed during lights-on phase show severe weight loss when exposed to prolonged fasting

We also recorded the bodyweight at each sacrifice timepoint: food anticipation (after 16 h fast, when mice expect to be fed, Fig. 1, “A”), food intake (4 h after food was added, Fig. 1, “F”) and postprandial period (4 h after food was removed, Fig. 1, “P”) on all sacrifice days. The earliest sacrifice was done 3 days after the feeding shift (Day 3), followed by 7 (Day 7) and 14 days (Day 14) post-shift.

We then compared these sacrifice weights to pre-TRF values (Fig. 2B, dotted line). Surprisingly, on all sacrifice days, DF and SDF female mice showed a severe weight loss after 16 h fasting, reaching or even dipping below the pre-TRF weight (Fig. 2B, upper panel, Food anticipation), meaning that during a single fasting period these mice lost almost all of the weight gained over past 2-4 weeks. However, the fasting weight did become slightly more stable over time. In contrast, male mice were less likely to drop below the pre-TRF weight after 16 h fasting (Fig. 2B, lower panel, Food anticipation).

Weights at the food intake timepoint (Fig. 2B, Food intake) tended to increase over time, especially in male mice. This supports our observation that adjustment to the new TRF regime is not immediate. Mice from all TRF groups also seemed to consume similar amounts of food, as there were no significant weight differences between the various feeding groups.

Fasting blood glucose increases in female mice fed from ZT4 to ZT12

Fasting blood glucose was measured at the food anticipation timepoint (Fig. 2, “A”). We observed that female mice struggled to quickly adjust to day feeding. On sacrifice Day 3, female DF mice showed significantly lower fasting blood glucose levels, while SDF mice showed a trend for an increased blood glucose (p=0.06), when compared to NF controls (Fig. 2C). A similar trend was observed on sacrifice Day 7, but by Day 14, DF mice were no longer different from NF controls (Fig. 2C, in yellow). Fasting glucose levels in SDF mice, however, did not show any change over time and remained slightly elevated (p=0.056) until the end of the study (Fig. 2C, in orange).

Male mice did not exhibit the exact same fasting glucose pattern. Shifting the food intake to ZT16-ZT24 significantly lowered fasting blood glucose levels for at least 7 days post-shift (Fig. 2C, right panel, in black). Similar to observations in female mice, food intake during ZT4-ZT12 slightly raised (p=0.06) the glucose levels in males, however here it tended to decrease over time, reaching NF-like levels by Day 14 (Fig. 2C, right, in orange).

It appears that food intake during the late lights-on phase (ZT4-ZT12) leads to a slight increase in fasting blood glucose levels in both sexes, while food intake during late lights-off phase (ZT16-ZT0) lowers glucose levels in male mice.

Food intake during the lights-on phase leads to lower transepithelial electrical resistance in ileal epithelia

Ileum from mice sacrificed during the food intake timepoint (Fig. 1, “F”) was used to determine transepithelial electrical resistance. All feeding groups showed similar TEER values on sacrifice Day 3 (Fig. 2D, Day 3), indicating lack of early response to the feeding shift. However, we did observe changes under prolonged TRF. Food intake between ZT12 and ZT20 led to a slight increase in TEER in both sexes, with males showing significant improvement in ileal resistance by Day 14 (Fig. 2D, in grey). Interestingly, the SNF group was the only one showing stable TEER value over time in both sexes (Fig. 2D, in black). If mice were fed during lights-on phase, TEER seemed to lower over time independently of the feeding shift (Fig. 2D, in yellow and orange), especially in male mice.

Overall, similar to observations regarding blood glucose levels and weight gain, the most detrimental effects were observed when the food intake was restricted to ZT4-ZT12.

Food-entrained gene expression in the digestive system

Gene expression in the digestive system shows three distinct response types to food entrainment

Expression of genes involved in molecular clock, nutrient metabolism, and immune response was determined in the liver, stomach corpus and duodenal mucosa. Tissue samples were collected from all experimental animals on sacrifice days 3, 7 and 14 (post-shift), at food anticipation, food intake, and postprandial timepoints (Fig. 1, “A”, “F” and “P”, respectively), and RNA was isolated. Gene expression was first normalised against housekeeping gene *18s* and then to the expression level in NF male mice at food anticipation timepoint on sacrifice Day 3.

In general, we observed three distinct gene expression responses to food intake time, summarized in Table 2 (ignoring sex- and timepoint-specific differences).

1) multiple tested genes did not show any difference in expression, so we classified these as “non-responsive”. 2) genes showing a change in expression between food anticipation and (one of) the other timepoints were classified under “diurnal response”. And 3) a significant gene population did show differences in expression due to the 4 h food intake shift. This difference could be observed in both diurnally non-responsive and responsive genes. Thus, in some cases we observed diurnal response together with a shift-driven up- or down-regulation of

gene expression, suggesting that food entrainment leads to a multi-tier regulation. All genes showing expression changes in response to the feeding shift, independently of their diurnal response, were classified under “baseline change”. Interestingly, only in the stomach all diurnally responsive genes also underwent a baseline change.

Table 2. Summary of gene expression responses to food-entrainment. Data from all sacrifice days pooled, ignoring sex-specific differences.

Organ	Non-responsive genes	Diurnal response	Baseline change
Liver	*Tas1r2* *Pept1, B^0at1* *Il-17a, Il-6, Crp, Igf-1*	*Bmal1, Clock* *Glut2, Gys2, Pepck* *Pparα, Fasn, Cyp7a1, Srebf1, Mttp* *Nampt* *Fgf21* *TNFα*	*Bmal1, Clock* *Glut2, Sglt1, Gys2, Pepck* *Pparα, Mttp, Fasn, Srebf1* *Nampt* *TNFα, Gpx1*
Stomach	*Tas1r2, Sglt1, Glut2* *Pept1, B^0at1* *Mttp, Fasn, Cyp7a1* *Il-17a*	*Bmal1, Clock* *Pepck* *Pparα* *Tph1, Gast, Sst, Lepr, Pga5, Ghrl* *Il-6, Gpx2, TNFα*	
Duodenum	*Cyp7a1, Mttp, Fasn* *Sst, Ghrl* *Il-6, Il-17a*	*Bmal1, Clock* *Tas1r2, Sglt1, Glut2, Pepck* *Pept1, B^0at1* *Pparα* *Gip, Gcg, Cck, Tph1* *Gpx2, TNFα*	*Bmal1, Clock* *Tas1r2, Glut2, Sglt1, Pepck* *Pept1, B^0at1* *Pparα* *Gip, Gcg, Cck, Tph1* *TNFα*

Colours mark different assigned groups by gene product function: light blue – core clock genes; purple – glucose sensing, transport, and metabolism; orange – lipid metabolism; pink – biosynthesis of NAD+; red – amino acid and peptide transport, green – hormone signalling; grey – pro-/anti-inflammatory response.

Food intake time entrains digestive clocks in an organ-specific manner

To determine whether the chosen TRF regimes were able to uncouple and reset peripheral clocks, we looked at the expression of clock genes *Bmal1* and *Clock* in the liver, stomach and duodenum. In all tested organs, *Bmal1* showed a stronger diurnal response than *Clock*, indicating possible uncoupling of *Bmal1-Clock* dimer (Fig. 3) «Insert Fig. 3». Even in NF mice, *Clock* showed low relative expression and barely any change in expression between the chosen timepoints (Fig. 3, NF). This was a quite unexpected result, as night feeding is expected to mimic the natural food intake period in mice the closest, aligning with the central, light-entrained clock, and thus is not expected to disrupt the diurnal rhythmicity of peripheral clock genes.

The response to TRF was also highly organ-specific. Livers of both DF and SDF mice showed an overall lower expression of both clock genes (Fig. 3, top panel), when compared to their night-fed counterparts. In stomach and duodenum, we observed the opposite (Fig. 3 mid- and bottom panels), accompanied by loss of diurnal rhythmicity of *Bmal1*.

In addition, sex-specific differences in TRF-dependent regulation were present as well. In both NF and DF female mice hepatic *Bmal1* showed weakening of diurnal response over time, however this could be rescued by the corresponding 4 h feeding shift (Fig. 3, top left panel). In male mice, the hepatic *Bmal1* diurnal

response tended to strengthen or remain unchanged over time in almost all feeding groups (Fig. 3, top right panel). Similar diurnal response pattern with females showing a strong early response and males showing stronger responses over time, was also observed for hepatic *Clock* and duodenal *Bmal1* expression. Interestingly, in the stomach *Bmal1* diurnal expression showed the opposite sex-specific pattern: under prolonged TRF, rhythmicity weakened in males, but not in females.

As evident by these conflicting responses, TRF was not able become the dominant zeitgeber for clock genes in all tested digestive organs, leading to a highly organ- and sex-specific regulation instead.

Food intake during the lights-on phase downregulates hepatic gene expression, while TRF between ZT16 and ZT0 elicits diurnal responses

Similar to our observations with clock genes, hepatic nutrient metabolism- and inflammatory response-related genes showed an overall lower expression in DF and SDF mice of both sexes (Fig. 4) «Insert Fig. 4». In addition, even though multiple genes did show a difference in expression between the timepoints, the overall diurnal response to daytime feeding was poor, suggesting that these TRF regimes were unable to fully uncouple the local hepatic clocks from the central clock-driven regulation.

TRF during the early lights-off phase (ZT12-ZT20) was not able to induce strong and persistent diurnal responses either. For example, *Pparα* and *Srebf1*, the principal transcription factors regulating hepatic lipid metabolism, showed almost no diurnal rhythmicity in their gene expression (Fig. 4), especially in female mice. Over time some rhythmicity appeared under SNF, DF and even SDF, indicating that these genes are at least partially responsive to food intake, just not under NF. Poor rhythmicity in *Pparα* and *Srebf1* expression could negatively affect the diurnal response of the whole lipid metabolism, and thus explain the lack of stable diurnal and baseline expression changes in genes involved in hepatic lipid secretion (*Mttp*) and cholesterol catabolism (*Cyp7α1*).

However, not every gene associated with lipid metabolism was so unresponsive to TRF. Gene encoding fatty acid synthase (*Fasn*) showed a strong diurnal response in both sexes under SNF, with early rhythm being present also in NF and DF females, and late response present in NF males. Similarly, a gene encoding nicotinamide adenine dinucleotide (NAD^+) biosynthetic enzyme (*Nampt*), which is involved in cellular energy metabolism, including fatty acid oxidation (Amjad et al., 2021), was responsive to TRF during lights-off phase as well.

The most robust diurnal rhythmicity in the liver was shown by a gene encoding fibroblast growth factor 21 (*Fgf21*). This gene is secreted during fasting and

involved in the regulation of nutrient and energy homeostasis (Flippo and Potthoff, 2021), therefore its rhythmicity was likely entrained by the daily 16 h fasting periods our mice experienced. Interestingly, we observed a shift in the nadir of *Fgf21* expression: in NF mice it was recorded at the food intake timepoint, while in all other feeding groups – at the postprandial period, hinting towards potential differences in food consumption pattern.

Food intake time seemed to affect the dip in *Fgf21* expression, shifting it from the food intake period in NF mice into postprandial period in almost all other mice groups.

As the liver plays a major role in glucose metabolism and storage, we also looked at the gene expression of key players in these processes. Almost no diurnal responses were observed for genes encoding glucose transporters (*Glut2, Sglt1*), nevertheless persistent rhythm was present for genes involved in regulation of glycogen synthesis (*Gys2*) and gluconeogenesis (*Pepck*), especially under SNF. Not much is known about the diurnal regulation of peripheral inflammation. Unfortunately, we only observed poor, inconsistent diurnal responses in the tested genes, with male mice likely to show a peak expression of *TNF*α during food intake timepoint.

Overall, SNF (ZT16-ZT20) appeared to be the most effective zeitgeber in the liver, leading to diurnal responses in multiple tested genes. Following the

observations on clock genes, female mice were more likely to show early responses, but male mice – late ones. These data imply that male livers require longer entrainment, however once a response is formed, it seems to be more persistent than in female mice.

TRF is a poor zeitgeber in the stomach

The gastrointestinal tract, including the stomach and duodenum, is directly exposed to the ingested food, thus one would expect its function to be highly adaptive to nutrient-derived signals. Surprisingly, in our study the stomach was the least responsive organ to TRF. Most of the tested genes did not show any diurnal response in their expression, especially in female mice (Fig. 5) «Insert Fig. 5». The food intake during the lights-on phase caused an overall gene upregulation (Fig. 5, DF, SDF), following the pattern seen for the gastric clock genes (Fig. 3), but opposing our observations in the liver (Fig. 4).

Genes encoding major GI hormones or their precursors, such as *Ghrl, Sst, Pga5* and *Lepr* (encodes leptin receptor), all showed similar expression patterns with a weak diurnal rhythm appearing after prolonged NF (females), SNF (both sexes) or DF (males).

A diurnal expression pattern was observed for *Gast* gene encoding gastrin, a hormone stimulating gastric acid release and GI motility. Although its function is essential for nutrient digestion, the rhythmicity was highly chaotic, appearing and

disappearing under various feeding conditions. Some studies have suggested that *Pparα* could regulate *Gast* expression and/or translation, indicating that they might belong to the same regulatory pathway (Saha, 2015; Bakke et al., 2002). However, we observed no similarities between their expression patterns. A similar, chaotic diurnal response was also seen for *Tph,* which encodes rate limiting protein in serotonin synthesis. We hypothesize that such chaotic and unstable responses might arise due to multiple environmental inputs, that often do not align. Still, it is unclear why this major digestive organ is so poorly entrained by food intake.

Strong sex-specificity and slow diurnal rhythm formation were present for genes encoding (anti-)inflammatory markers *Gxp2*, *Il-6* and *TNFα*. While in female mice the changes in gene expression were negligible, prolonged DF was able to induce (*Gxp2, TNFα*) or sustain (*Il-6*) diurnal responses in male mice, implying that food intake in daytime might cause gastric inflammation.

The gene showing the strongest diurnal rhythmicity was a surprising find. *Pepck*, encoding a rate-limiting enzyme for gluconeogenesis, showed a robust rhythm under SNF. NF females and daytime-fed males showed strong *Pepck* diurnal rhythmicity as well, with peak expression occurring at food anticipation. Apart from the liver, gluconeogenesis has been shown to occur in the small intestine (Troy et al., 2008), especially after gastric bypass surgery (Vily-Petit et al., 2022),

but currently there is no evidence for glucose production in the stomach. Perhaps, this strong diurnal regulation of gastric *Pepck* could be connected with its proposed role in the Krebs cycle (Montal et al., 2015). We observed a robust *Pepck* rhythm also in the liver (Fig. 4), therefore we cannot exclude a presence of an inter-organ signalling that regulates its expression systematically.

Duodenal genes involved in nutrient metabolism are strongly entrained by TRF

The duodenum is responsible for further digestion and absorption of nutrients; thus, food intake and nutrient-related signals would be expected to regulate its gene expression. We observed several similarities in gene expression patterns between stomach and duodenum. First, daytime feeding led to an overall gene upregulation (Fig. 6, DF, SDF) «Insert Fig.6». Second, the genes encoding GI hormones or their precursors (*Cck, Gip, Ccg, Tph1*) showed poor rhythmicity. However, most of the tested duodenal genes were highly responsive to TRF, especially to NF.

Robust diurnal rhythm was seen for genes encoding large amino acid (B^0*at1*) and peptide (*Pept1*) transporters under all tested conditions. Interestingly, here male mice did show an early response that weakened over time, and females had stronger late responses, opposite to our observations in the liver. Similar, sometimes almost identical, expression patterns to B^0*at1* and *Pept1* were shown

also by *Ppar*α, *Sglt1* (encodes a major glucose transporter), *Tas1r2* (encodes a sweet taste receptor) and, unexpectedly, the anti-inflammatory marker *Gxp2,* suggesting that their diurnal regulation might occur via the same signalling pathway. In contrast, another gene encoding glucose transporter (*Glut2*) showed a poor diurnal response, suggesting that its diurnal regulation is independent of other tested glucose metabolism regulating genes.

Gene *Pepck*, which had demonstrated a strong diurnal response the liver (Fig. 4) and stomach (Fig. 5), showed adaptation to TRF duodenum as well, especially in male mice. It is intriguing, that *Pepck* developed robust diurnal rhythms in all tested organs, something that was not observed even for *Clock* gene. This implies that *Bmal1-Clock* signalling is not required for development of all local diurnal rhythms and that food entrainment is highly gene-specific.

Discussion

This study describes how food intake time affects weight gain, fasting glucose levels, intestinal permeability, and the expression of peripheral clock and nutrient metabolism-related genes in the digestive system of male and female mice. We utilized TRF model to limit the food consumption to 8 h in a 24 h period, with the initial experimental groups starting their feeding period either at ZT12 (NF) or ZT0 (DF). After 14 days of entrainment, food intake time was shifted 4 h forward in half of the mice (Fig. 1). Observed changes in physiological parameters (relative to NF controls) have been summarized in Table 3.

Table 3. Changes in physiological parameters due to prolonged food-entrainment, relative to NF controls

Feeding groups	**Weight gain**		**Fasting blood glucose**		**TEER**	
	Females	*Males*	*Females*	*Males*	*Females*	*Males*
Night-fed (NF)	highest	Lowest	No change over time		Increases over time	
Shifted night-fed (SNF)	-	-/↑	-	↓	-	-
Day-fed (DF)	-/↓	-	-	-	-/↓	↓
Shifted day-fed (SDF)	↓	↑	-/↑	-	↓	↓↓

We observed remarkable sex-specific differences in weight gain, with males and females often showing an opposite response to the same TRF regime (Fig. 2A).

Food intake during the lights-on phase led to an overall lowest weight gain in females, independently of the 4 h feeding shift; while males had their lowest weight gain under NF, but increased weight due to any of the 4 h feeding shifts. Lack of impact of DF on weight gain in male mice has been observed before (Jang et al., 2012; Acosta-Rodríguez et al., 2017); however, to our knowledge, there are no studies focusing on weight gain in female mice under TRF.

We also observed that DF and SDF mice, especially females, lost a significant amount of weight during a single 16 h fasting period, even after prolonged entrainment (Fig. 2B). We hypothesise that these mice struggled to adjust to the new food intake time, possibly staying active in the lights-off period when they were unable to replenish the lost calories. There have been suggestions that the regulation of physical activity is fairly complicated, involving both the central clock and the feedback from food-entrained oscillators (Dattolo et al., 2016). Therefore, additional measurements of locomotion and central clock activity would be needed to assess their sex-specificity and role in weight gain under various TRF regimes.

Regulation of blood glucose levels was similar in both sexes, leading to hyperglycaemia when food intake was shifted to the late lights-on phase (ZT4 – ZT12) (Fig. 2C). Higher fasting blood glucose levels in DF mice have been observed before (Mukherji et al., 2015), and studies with rats have detected poor

glucose tolerance under daytime feeding (de Goede et al., 2019). However, it has also been shown that mice on the standard 12 h LD cycle reach the blood glucose peak during the first half of lights-on phase (ZT0-ZT4) (Jensen et al., 2013), that coincides with the glucose measurement time in our SDF mice (ZT4). Thus, it is also possible, that the observed higher glucose levels in SDF mice reflect the light-driven rhythm of glucose clearance.

The disruption of the intestinal barrier and epithelial resistance has been understudied in the context of food entrainment. Studies with mouse colitis models have shown that TRF during the dark phase leads to an upregulation of tight junction protein expression, allowing to preserve intestinal integrity (Zhang et al., 2020). Our data support these observations, demonstrating an increase in TEER under prolonged NF in both sexes (Fig. 2D). It has also been shown that the intestinal permeability increases in constant lights-on environment (Deaver et al., 2018) and due to LD cycle shifts (Tran et al., 2021), aligning with our observed reduction in TEER in DF and SDF mice, implying increased intestinal leakiness.

Overall, our data suggest that both glucose handling and intestinal permeability show poor adjustment to daytime feeding. At the same time, if TRF is applied during the lights-off phase, these physiological functions can improve. Clearly, an alignment between light-driven regulation and peripheral zeitgebers is necessary to preserve glucose tolerance and intestinal barrier function.

Regarding the nutrient-metabolism related gene expression, we observed two seemingly independent types of regulation, both highly sex- and organ-specific: 1) a change in expression levels due to the 4 h feeding shift (=baseline change); and 2) differences between the timepoints within the same feeding condition (=diurnal response). There has not been much focus on non-diurnal responses to TRF, but organ- and sex-specificity has already been observed in multiple studies (for reviews see (Doherty and Kay, 2010; Krizo and Mintz, 2015), raising an interest in systems-level circadian regulation. In our study, organ and sex-specificity was especially evident in the expression of local clock genes *Clock* and *Bmal1*, where daytime feeding led to a downregulation in liver, but upregulation in stomach and duodenum (Fig. 3). In addition, the liver (Fig. 4) and stomach (Fig. 5) of female mice were more likely to show an early rhythmicity that dissipated over time, while in males the rhythm strengthened. This pattern was reversed in the duodenum (Fig. 6). Our observations suggest that in the upper GI tract: a) TRF is not able to fully uncouple local clocks; b) daytime feeding causes persistent upregulation of *Bmal1-Clock* expression, potentially affecting their target transcription; c) the entrainment speed and stability is sex- and organ-specific.

Our observations have also shown that a single TRF regime is unable to entrain and synchronize diurnal rhythms across the digestive system. However, this does

not imply a total absence of inter-organ communication in peripheral entrainment. For example, we observed that gene *Pepck*, encoding phosphoenolpyruvate carboxykinase, showed robust rhythms in all tested organs, especially under SNF (Figs. 4-6). Gene-specific responses to TRF were quite common in our study, even if the genes belonged to the same metabolic pathway; e.g., *Fgf21* exhibited a strong diurnal rhythm in the liver, despite its upstream regulator *Ppar*α (Badman et al., 2007) being largely unresponsive to TRF (Fig. 4). We therefore wonder whether zeitgeber signals might be integrated on a gene level, undermining the existence of a single food-entrainable oscillator and the strict master-peripheral clock hierarchy.

The suprachiasmatic nucleus (SCN) is thought to be the main coordinator of the light-entrained circadian rhythms, initiating and/or synchronizing oscillations also in peripheral clock genes, giving SCN the role of the master circadian regulator (Tokuda et al., 2018; Hastings et al., 2018; Mieda, 2020). However, we are not alone in suggesting a more complicated interaction between central and peripheral clocks that would require an assessment and integration of all zeitgeber signals, independently of their origin. The master clock role of the SCN has been questioned before, as studies have shown persistent circadian rhythms in explants of adipose tissue, lung, liver, and kidney (Gómez-Santos et al., 2009; Yoo et al., 2004). The neuronal activity in rat and mouse SCN has been observed

to be reduced under DF, allowing food anticipatory activity to occur during the passive, lights-on phase (Acosta-Galvan et al., 2011; Dattolo et al., 2016). Moreover, clock genes *Rev-erbα* and *Bmal1* in the SCN entrain to food-entrainment in rats kept in constant light (Novakova et al., 2011). Thus, it appears that peripheral signals might exert at least a modulatory effect on SCN, despite being seen as 'lesser' zeitgebers. It has also been shown that the application of various zeitgebers at once might lead to a system-level disruption of circadian rhythms, and a conflicting regulation, which would align with our observations (light phase vs. food intake). For example, while the physical activity and body temperature of mice on alternating light schedules did adjust to TRF during the lights-off phase, plasma triglyceride levels or energy expenditure did not (Schilperoort et al., 2019). Another study observed that 4 weeks of TRF seemed to reduce inflammation in jejunum; however, an additional supplementation of an anti-inflammatory vitamin A analog ATRA (all-*trans* retinoic acid), led to an unexpected increase in several pro-inflammatory and disease markers (Sherman et al., 2011). ATRA acted as a zeitgeber itself, generating a rhythm that did not align with the chosen TRF regime (Sherman et al., 2012), thus the application of these two anti-inflammatory treatments led to a circadian incoherence on systemic level, instead of expected synergistic reduction of inflammation.

This, of course, raises the question of how diurnal rhythmicity can emerge in presence of conflicting zeitgebers. It has been suggested that circadian clocks can be divided into weak and strong oscillators. Based on tests with explants of lung tissue and SCN, peripheral tissue seems to act as a weak oscillator, achieving larger phase shifts and easily aligning their amplitude. SCN seems to be a strong oscillator, entraining within narrower ranges, unaffected by the period of zeitgeber (Abraham et al., 2010). However, if multiple weak oscillators (e.g., various organs/tissues) are coupled, they act as a single strong oscillator as well (Abraham et al., 2010; Schmal et al., 2018; Gonze et al., 2005). Therefore, peripheral organs are more sensitive to entrainment, however, diurnal rhythms on systemic level will only emerge when multiple zeitgebers align.

The existence of weak and strong clocks and the complex interaction of various zeitgebers could explain organ-and gene-specific TRF responses described in our study. While specific food intake regimes might synchronize gene expression rhythms within the same organ, TRF will not achieve a full systemic synchronization alone. Instead, circadian regulation will happen by integration of all present zeitgeber signals.

Untangling the level at which this regulation happens (A single gene? Or gene groups?) would require a large-scale study, using aligning vs. conflicting zeitgebers and looking at expression/activity of upstream and downstream

effectors within the same signalling pathway across multiple organs. As sex-specific diurnal regulation seems to be broadly present in the periphery as well, all future circadian studies assessing the impact of shift work, sleep disturbances, time zone changes, and chronotherapies should utilize experimental models representing both sexes. Overall, our study has shown that the complexity and specificity of the peripheral diurnal regulation can only be revealed in multi-organ studies, looking at various response types.

Acknowledgements

We thank Single Cell and High Throughput Genomics Platform at Monash Health Translation project, especially Dr. Sen Wang, for performing the IFC analysis. We also thank Prof. Frédéric Gachon from the Institute of Bioscience at University of Queensland for the constructive exchange regarding experimental approaches and methodology.

Competing interests

The authors of this study confirm there are no competing interests.

Author contributions

All experiments were carried out at the Department of Anatomy and Physiology, The University of Melbourne and the Florey Institute of Neuroscience and Mental

Health. L.O-R., M. R. di N., R.M. and J.B.F designed the study and necessary experiments. M. R. di N., L.O-R., R.M., B.H., A.K., M.R., T.E.F.C. and L.J.F carried out the experiments. L.O-R., M.R. di N., R.M and J.B.F. analysed and interpreted the data. L.O-R., M.R. di N., R.M. and J.B.F. wrote and critically revised the manuscript. All authors approved the final version of the manuscript. All persons qualifying for authorship are listed as such.

Funding

This study was supported by the Swiss National Science Foundation Grant No. 187739 to L.O-R.

References

Abraham U, Granada AE, Westermark PO, et al. (2010) Coupling governs entrainment range of circadian clocks. *Molecular Systems Biology* 6(1): 438.

Acosta-Galvan G, Yi C-X, Vliet vdJ, et al. (2011) Interaction between hypothalamic dorsomedial nucleus and the suprachiasmatic nucleus determines intensity of food anticipatory behavior. *Proc Natl Acad Sci USA* 108(14): 5813-5818.

Acosta-Rodríguez VA, de Groot MHM, Rijo-Ferreira F, et al. (2017) Mice under Caloric Restriction Self-Impose a Temporal Restriction of Food Intake as Revealed by an Automated Feeder System. *Cell Metabolism* 26(1): 267-277.e262.

Aguayo A, Martin CS, Huddy TF, et al. (2018) Sex differences in circadian food anticipatory activity are not altered by individual manipulations of sex hormones or sex chromosome copy number in mice. *PLOS ONE* 13(1): e0191373.

Albrecht U (2012) Timing to Perfection: The Biology of Central and Peripheral Circadian Clocks. *Neuron* 74(2): 246-260.

Amjad S, Nisar S, Bhat AA, et al. (2021) Role of NAD(+) in regulating cellular and metabolic signaling pathways. *Mol Metab* 49: 101195.

Aschoff J (1945) Zeitgeber der tierischen Tagesperiodik. *Naturwissenschaften* 41: 49-56.

Asher G and Sassone-Corsi P (2015) Time for food: the intimate interplay between nutrition, metabolism, and the circadian clock. *Cell* 161(1): 84-92.

Badman MK, Pissios P, Kennedy AR, et al. (2007) Hepatic Fibroblast Growth Factor 21 Is Regulated by PPARα and Is a Key Mediator of Hepatic Lipid Metabolism in Ketotic States. *Cell Metabolism* 5(6): 426-437.

Bakke I, Hammer TA, Sandvik AK, et al. (2002) PPAR alpha stimulates the rat gastrin-producing cell. *Mol Cell Endocrinol* 195(1-2): 89-97.

Balakrishnan A, Stearns AT, Ashley SW, et al. (2010) Restricted feeding phase shifts clock gene and sodium glucose cotransporter 1 (SGLT1) expression in rats. *J Nutr* 140(5): 908-914.

Begemann K, Neumann A-M and Oster H (2020) Regulation and function of extra-SCN circadian oscillators in the brain. *Acta Physiol (Oxf)* 229(1): e13446.

Buhr E and Takahashi J (2013) Molecular components of the mammalian circadian clock. *Handb Exp Pharmacol* 217: 3-27.

Buijs F, Leon-Mercado L, Guzman-Ruiz M, et al. (2016) The circadian system: a regulatory feedback network of periphery and brain. *Physiology* 31(3): 170-181.

Cox K and Takahashi J (2019) Circadian clock genes and the transcriptional architecture of the clock mechanism. *J Mol Endocrinol* 63(4): R93-R102.

Crawford M and Thor D (1964) Circadian activity and noise comparisons of two confined groups with and without reference to clock time. *Percept Mot Skills* 19: 211-216.

Crowley S and Eastman C (2018) Free-running circadian period in adolescents and adults. *J Sleep Res* 27(5): DOI: 10.1111/jsr.12678

Damiola F, Le Minh N, Preitner N, et al. (2000) Restricted feeding uncouples circadian oscillators in peripheral tissues from the central pacemaker in the suprachiasmatic nucleus. *Genes & development* 14(23): 2950-2961.

Dattolo T, Coomans CP, van Diepen HC, et al. (2016) Neural activity in the suprachiasmatic circadian clock of nocturnal mice anticipating a daytime meal. *Neuroscience* 315: 91-103.

de Goede P, Foppen E, Ritsema WIGR, et al. (2019) Time-Restricted Feeding Improves Glucose Tolerance in Rats, but Only When in Line With the Circadian Timing System. *Frontiers in Endocrinology* 10.

Deaver JA, Eum SY and Toborek M (2018) Circadian Disruption Changes Gut Microbiome Taxa and Functional Gene Composition. *Frontiers in Microbiology* 9.

Doherty CJ and Kay SA (2010) Circadian control of global gene expression patterns. *Annual review of genetics* 44: 419-444.

Duez H and Staels B (2008) The nuclear receptors Rev-erbs and RORs integrate circadian rhythms and metabolism. *Diab Vasc Dis Res* 5(2): 82-88.

Eastman C, Tomaka V and Crowley S (2016) Circadian rhythms of European and African-Americans after a large delay of sleep as in jet lag and night work. *Sci Rep* 6(36716): DOI: 10.1038/srep36716

Flippo KH and Potthoff MJ (2021) Metabolic Messengers: FGF21. *Nat Metab* 3(3): 309-317.

Fluidigm (2015) *Gene Expression with the 192.24 IFC Using Fast TaqMan Assays (Biomark HD only)*. Available at: https://fluidigm.my.salesforce.com/sfc/p/#700000009DAw/a/4u0000019jzR/7DaOMZh8GOtlvivpWQ5SIX5Xj9wPhQx9c1D4yMF0nVc.

Forni D, Pozzoli U, Cagliani R, et al. (2014) Genetic adaptation of the human circadian clock to day-length latitudinal variations and relevance for affective disorders. *Genome Biol* 15(10): DOI: 10.1186/s13059-13014-10499-13057

Gillman A, Rebec G, Pecoraro N, et al. (2019) Circadian entrainment by food and drugs of abuse. *Behav Processes* 165: 23-28.

Goetzl F and Stone F (1947) Diurnal variations in acuity of olfaction and food intake. *Gastroenterology* 9(4): 444-453.

Gómez-Santos C, Gómez-Abellán P, Madrid JA, et al. (2009) Circadian rhythm of clock genes in human adipose explants. *Obesity (Silver Spring)* 17(8): 1481-1485.

Gonze D, Bernard S, Waltermann C, et al. (2005) Spontaneous synchronization of coupled circadian oscillators. *Biophys J* 89(1): 120-129.

Hastings M, Maywood E and Brancaccio M (2018) Generation of circadian rhythms in the suprachiasmatic nucleus. *Nat Rev Neurosci* 19(8): 453-469.

Jang H, Lee G, Kong J, et al. (2012) Feeding Period Restriction Alters the Expression of Peripheral Circadian Rhythm Genes without Changing Body Weight in Mice. *PLOS ONE* 7(11): e49993.

Jensen T, Kiersgaard M, Sørensen D, et al. (2013) Fasting of mice: a review. *Laboratory Animals* 47(4): 225-240.

Kleitman N and Engelman T (1947) Diurnal cycle in activity and body temperature of rabbits. *Fed Proc* 6(1): 143.

Krizo JA and Mintz EM (2015) Sex Differences in Behavioral Circadian Rhythms in Laboratory Rodents. *Frontiers in Endocrinology* 5.

Kuroda H, Tahara Y, Saito K, et al. (2012) Meal frequency patterns determine the phase of mouse peripheral circadian clocks. *Sci Rep* 2(711): DOI:10.1038/srep00711.

Lewis P, Korf H, Kuffer L, et al. (2018) Exercise time cues (zeitgebers) for human circadian systems can foster health and improve performance: a systematic review. *BMJ Open Sport Exerc Med* 4(1): e000443.

Mellette H, Hutt B, Askovitz, SI and Horvath S (1951) Diurnal variations in body temperatures. *J Appl Physiol* 3(11): 665-675.

Mieda M (2020) The central circadian clock of the suprachiasmatic nucleus as an ensemble of multiple oscillatory neurons. *Neurosci Res* 156: 24-31.

Mills J (1951) Diurnal rhythm in urine flow. *J Physiol* 113(4): 528-536.

Mills J (1964) Circadian rhythms during and after three months in solitude underground. *J Physiol* 174: 217-231.

Montal ED, Dewi R, Bhalla K, et al. (2015) PEPCK Coordinates the Regulation of Central Carbon Metabolism to Promote Cancer Cell Growth. *Mol Cell* 60(4): 571-583.

Mukherji A, Kobiita A and Chambon P (2015) Shifting the feeding of mice to the rest phase creates metabolic alterations, which, on their own, shift the peripheral circadian clocks by 12 hours. *Proceedings of the National Academy of Sciences* 112(48): E6683-E6690.

Novakova M, Polidarova L, Sladek M, et al. (2011) Restricted feeding regime affects clock gene expression profiles in the suprachiasmatic nucleus of rats exposed to constant light. *Neuroscience* 197: 65-71.

Ramakrishnan R, Qin J, Jones RC, et al. (2013) Integrated Fluidic Circuits (IFCs) for digital PCR. *Methods Mol Biol* 949: 423-431.

Rodbard S (1947) Body temperature-arterial pressure relationship as a basis for physiological interpretation of diurnal rhythm. *Fed Proc* 6(1): 191.

Saha L (2015) Role of peroxisome proliferator-activated receptors alpha and gamma in gastric ulcer: An overview of experimental evidences. *World J Gastrointest Pharmacol Ther* 6(4): 120-126.

Schibler U, Gotic I, Saini C, et al. (2015) Clock-talk: Interactions between central and peripheral circadian oscillators in mammals. *Cold Spring Harb Symp Quant Biol* 80: 223-232.

Schilperoort M, van den Berg R, Dolle M, et al. (2019) Time-restricted feeding improves adaptation to chronically alternating light-dark cycles. *Sci Rep* 9(1): DOI: 10.1038/s41598-41019-44398-41597.

Schmal C, Herzog ED and Herzel H (2018) Measuring Relative Coupling Strength in Circadian Systems. *Journal of Biological Rhythms* 33(1): 84-98.

Sherman H, Frumin I, Gutman R, et al. (2011) Long-term restricted feeding alters circadian expression and reduces the level of inflammatory and disease markers. *J Cell Mol Med* 15(12): 2745-2759.

Sherman H, Gutman R, Chapnik N, et al. (2012) All-trans retinoic acid modifies the expression of clock and disease marker genes. *J Nutr Biochem* 23(3): 209-217.

Silver R (2018) Cells have sex chromosomes and circadian clocks: Implications for organismal level functions. *Physiology & Behavior* 187: 6-12.

Sirota J and Baldwin D, Villarreal, H (1950) Diurnal variations of renal function in man. *J Clin Invest* 29(2): 187-192.

Solt L, Kojetin D and Burris T (2011) The REV-ERBs and RORs: molecular links between circadian rhythms and lipid homeostasis. *Future Med Chem* 3(5): 623-638.

Takahashi J and Lowrey P (2000) Genetics of the mammalian circadian system: Photic entrainment, circadian pacemaker mechanisms, and posttranslational regulation. *Annual review of genetics* 34: 533-562.

Tokuda I, Ono D, Honma S, et al. (2018) Coherency of circadian rhythms in the SCN is governed by the interplay of two coupling factors. *PLoS Comput Biol* 14(12): e1006607.

Tran L, Jochum SB, Shaikh M, et al. (2021) Circadian misalignment by environmental light/dark shifting causes circadian disruption in colon. *PLOS ONE* 16(6): e0251604.

Troy S, Soty M, Ribeiro L, et al. (2008) Intestinal Gluconeogenesis Is a Key Factor for Early Metabolic Changes after Gastric Bypass but Not after Gastric Lap-Band in Mice. *Cell Metabolism* 8(3): 201-211.

Vily-Petit J, Barataud A, Zitoun C, et al. (2022) Intestinal gluconeogenesis shapes gut microbiota, fecal and urine metabolome in mice with gastric bypass surgery. *Scientific Reports* 12(1): 1415.

Voigt RM, Forsyth CB and Keshavarzian A (2019) Circadian rhythms: a regulator of gastrointestinal health and dysfunction. *Expert review of gastroenterology & hepatology* 13(5): 411-424.

Welsh DK, Takahashi JS and Kay SA (2010) Suprachiasmatic nucleus: cell autonomy and network properties. *Annu Rev Physiol* 72: 551-577.

Xie X, Kukino A, Calcagno HE, et al. (2020) Natural food intake patterns have little synchronizing effect on peripheral circadian clocks. *BMC Biology* 18(1): 160.

Yan L and Silver R (2016) Neuroendocrine underpinnings of sex differences in circadian timing systems. *J Steroid Biochem Mol Biol* 160: 118-126.

Yoo S-H, Yamazaki S, Lowrey PL, et al. (2004) PERIOD2::LUCIFERASE real-time reporting of circadian dynamics reveals persistent circadian oscillations in mouse peripheral tissues. *Proceedings of the National Academy of Sciences of the United States of America* 101(15): 5339-5346.

Zhang X, Zou Q, Zhao B, et al. (2020) Effects of alternate-day fasting, time-restricted fasting and intermittent energy restriction DSS-induced on colitis and behavioral disorders. *Redox biology* 32: 101535-101535.

Zimmet P, Alberti K, Stern N, et al. (2019) The Circadian Syndrome: is the Metabolic Syndrome and much more! *J Intern Med* 286(2): 181-191.

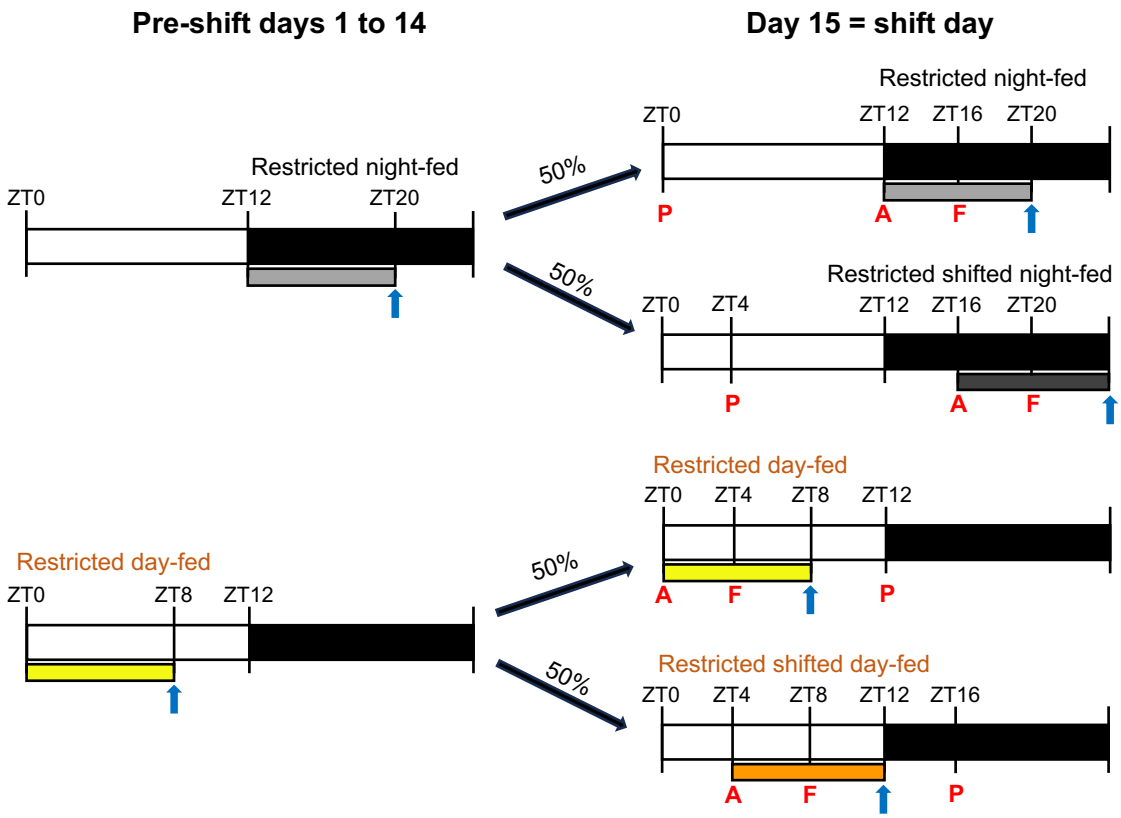

Figure 1. Food-entrainment groups. Bars indicate the placement and length of the feeding period. Arrows show weekly weight measurement timepoints. Mice were sacrificed on 3rd, 7th or 14th day post feeding shift. Letters indicate sacrifice timepoints on each day: A = food anticipation, F = food intake, P= postprandial. n = 5 per sacrifice timepoint per sex.

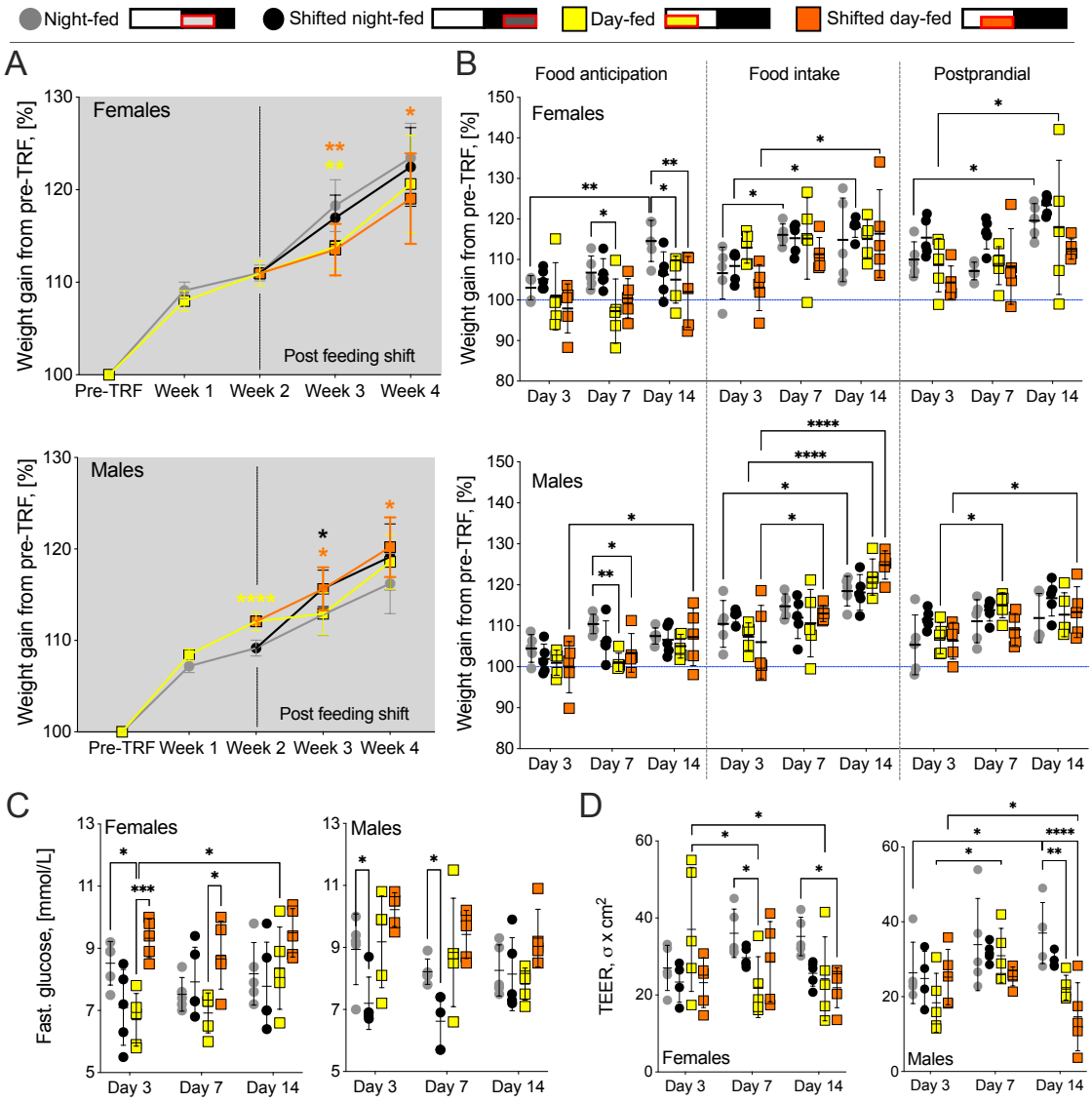

Figure 2. Physiological effects of time-restricted feeding regimes. A: Post-feeding weights were normalized to individual pre-food entrainment (pre-TRF) values. Mean (95% CI) shown, n = 90 mice per sex at pre-TRF, week 1 and week 2; week 3 n = 30 mice per sex; week 4 n = 15 mice per sex. Two-way ANOVA with Šidák's multiple comparison test (vs. night-fed group), *p<0.05,

p<0.01, ****p<0.0001. **B: Differences in recorded sacrifice weights. Values normalized to individual pre-food-entrainment (pre-TRF) values. **C**: Fasting glucose values recorded at food anticipation. **D**: Transepithelial electrical resistance in ileum, recorded at food intake. **B to D:** Mean (SD) shown, n = 5 mice per sex per timepoint. Two-way ANOVA with Dunnett's multiple comparison test, showing differences between feeding groups (night-fed as a control) and sacrifice days (Day 3 as a control), *p<0.05, **p<0.01, ***p<0.001, ****p<0.0001.

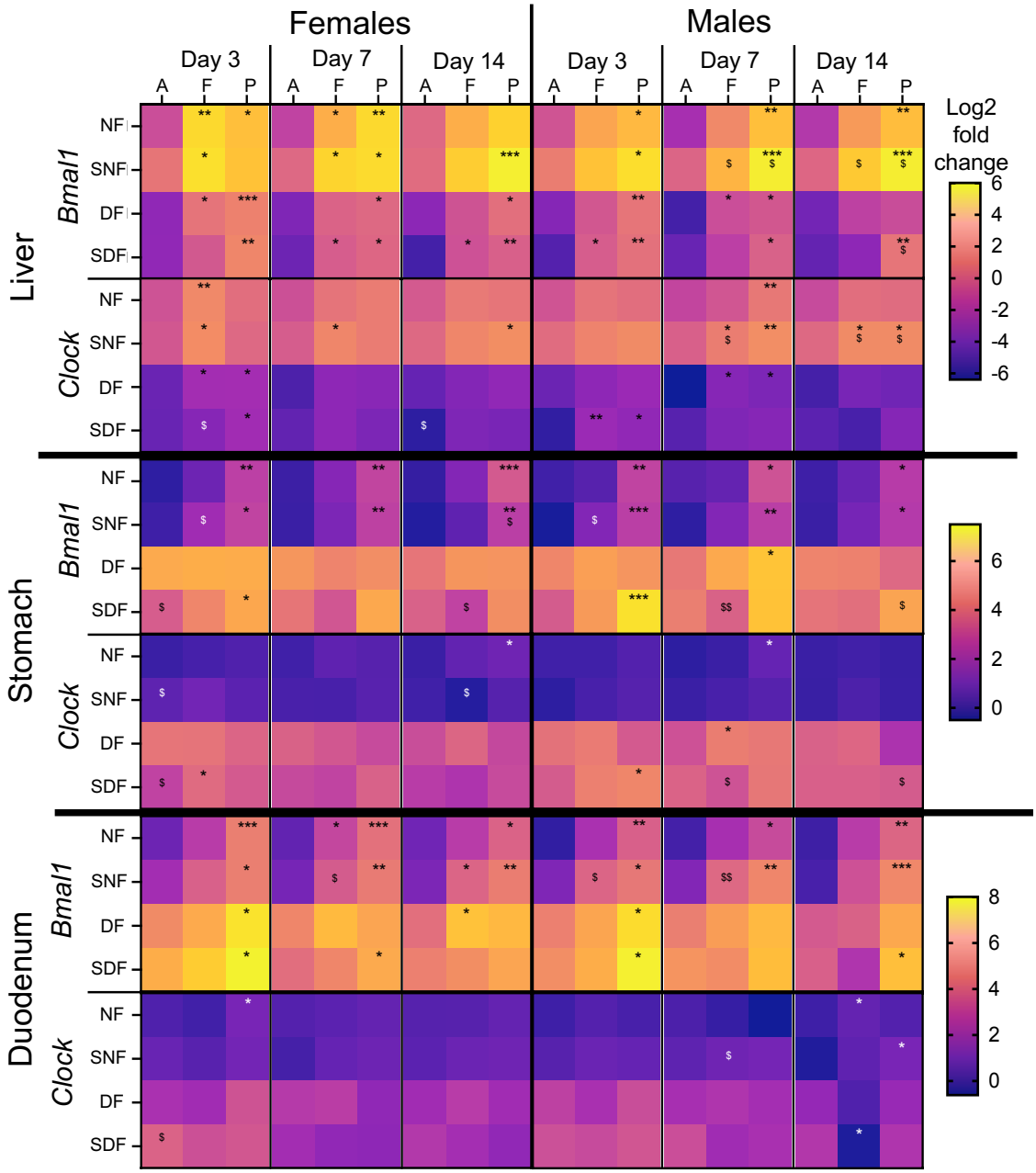

Figure 3. Changes in clock gene expression in liver, stomach and duodenum in response to food intake time. Sample collection timepoints shown at the top: A = food anticipation, F = food intake, P = postprandial period. Feeding conditions shown on the left: NF = night-fed (ZT12 – ZT20), SNF = shifted night-fed (ZT16 – ZT24), DF = day-fed (ZT0 – ZT8), SDF = shifted day-

fed (ZT4 – ZT12). Relative gene expression values (Log2) normalized to NF male mice on sacrifice day 3 at food anticipation timepoint and shown as means, n= 4-5 mice. Non-parametric Kruskal-Wallis test with Dunn's multiple comparison test used to show diurnal (vs. food anticipation) expression differences, *$p<0.05$, **$p<0.01$, ***$p<0.001$. The same test used to assess baseline differences (non-shifted vs. shifted) at each timepoint, $^{\$}p<0.05$, $^{\$\$}p<0.01$.

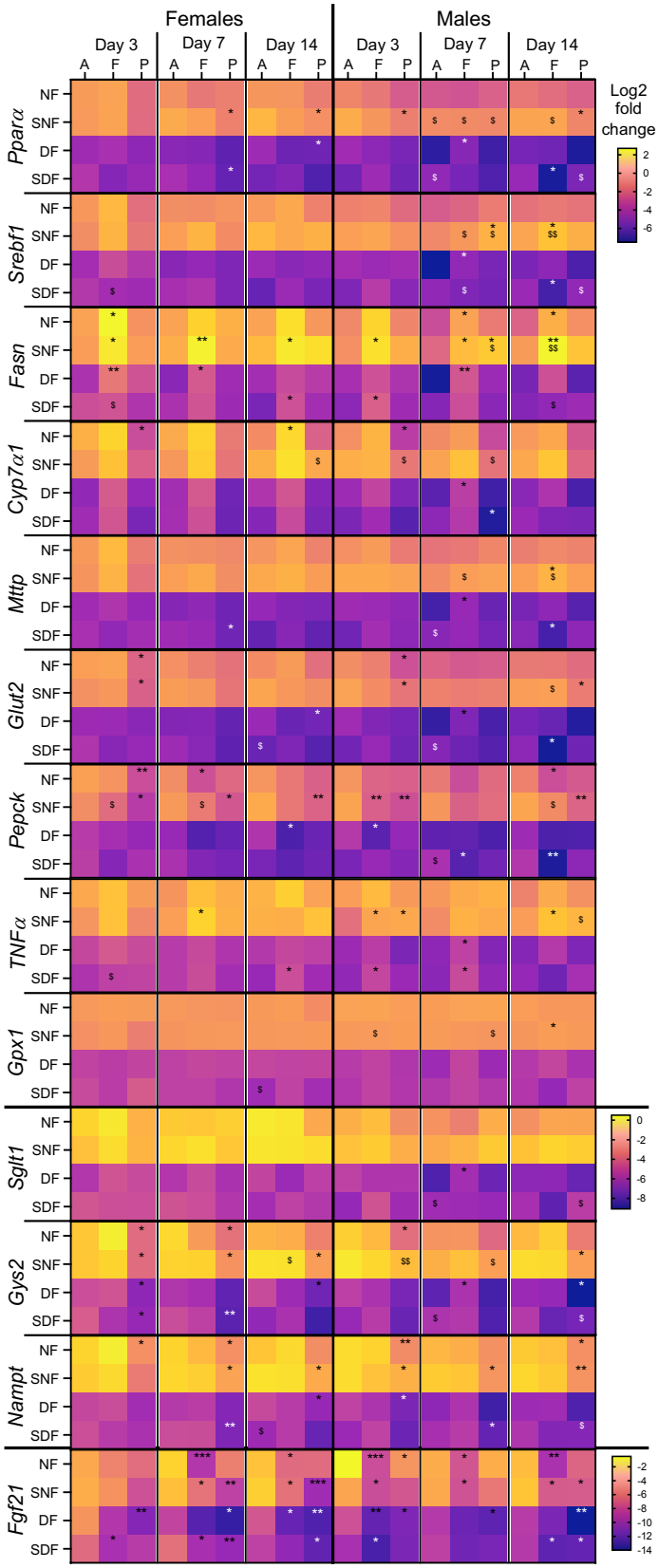

Figure 4. Hepatic diurnal and baseline gene expression changes in response to the food intake time. Sample collection timepoints shown at the top: A = food anticipation, F = food intake, P = postprandial period. Feeding conditions shown on the left: NF = night-fed (ZT12 – ZT20), SNF = shifted night-fed (ZT16 – ZT24), DF = day-fed (ZT0 – ZT8), SDF = shifted day-fed (ZT4 – ZT12). Relative gene expression values (Log2) normalized to NF male mice on sacrifice day 3 at food anticipation and shown as means, n= 4-5 mice. Non-parametric Kruskal-Wallis test with Dunn's multiple comparison test used to show diurnal (vs. food anticipation) expression differences, *p<0.05, **p<0.01, ***p<0.001. The same test used to assess baseline differences (non-shifted vs. shifted) at each timepoint, $p<0.05, $$p<0.01.

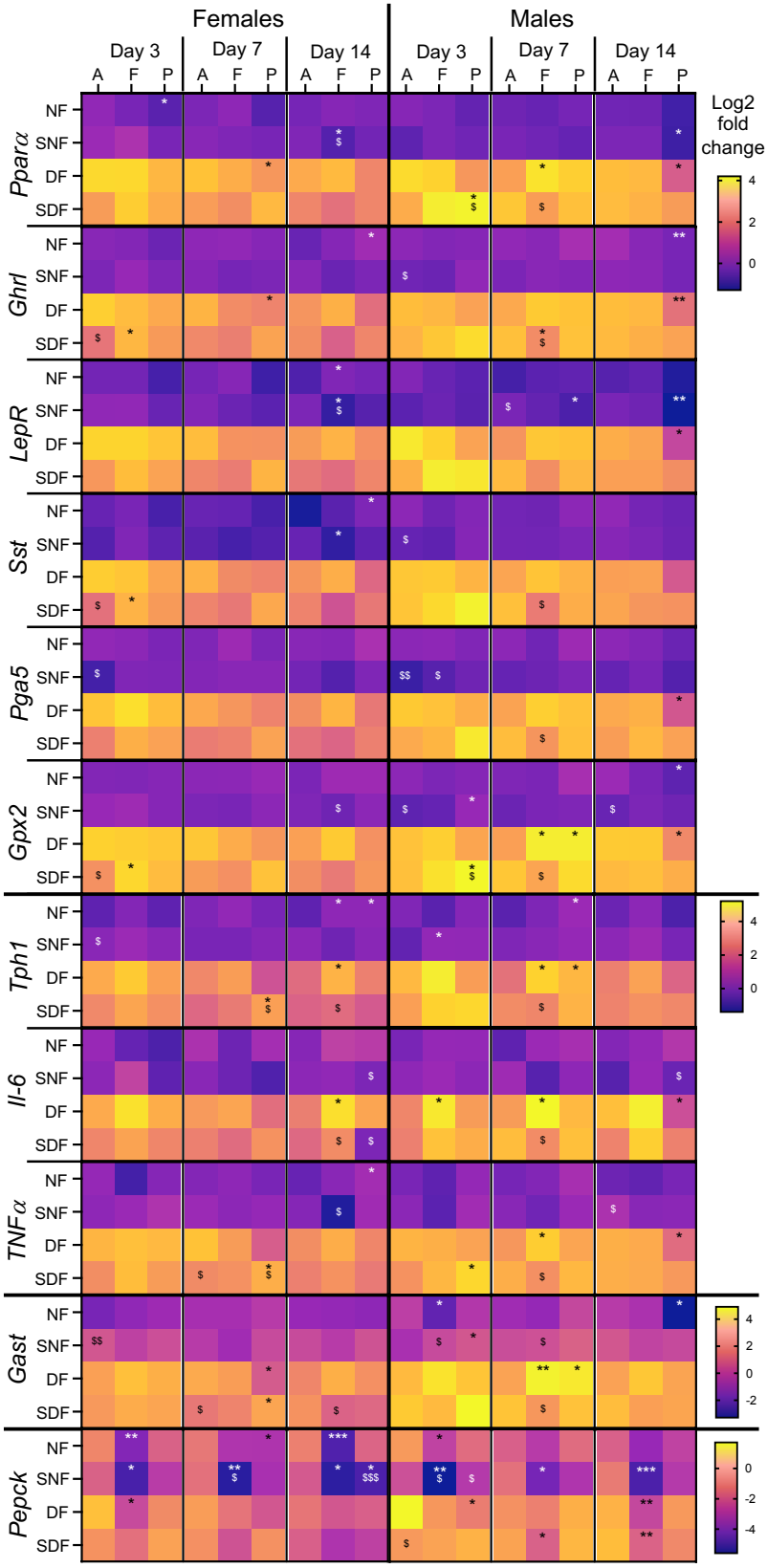

Figure 5. Diurnal and baseline gene expression changes in stomach in response to TRF. Sample collection timepoints shown at the top: A = food anticipation, F = food intake, P = postprandial period. Feeding conditions shown on the left: NF = night-fed (ZT12 – ZT20), SNF = shifted night-fed (ZT16 – ZT24), DF = day-fed (ZT0 – ZT8), SDF = shifted day-fed (ZT4 – ZT12). Relative gene expression values (Log2) normalized to NF male mice on sacrifice day 3 at food anticipation and shown as means, n= 4-5 mice. Non-parametric Kruskal-Wallis test with Dunn's multiple comparison test used to show diurnal (vs. food anticipation) expression differences, *p<0.05, **p<0.01, ***p<0.001. The same test used to assess baseline differences (non-shifted vs. shifted) at each timepoint, $p<0.05, $$p<0.01, $$$p<0.001.

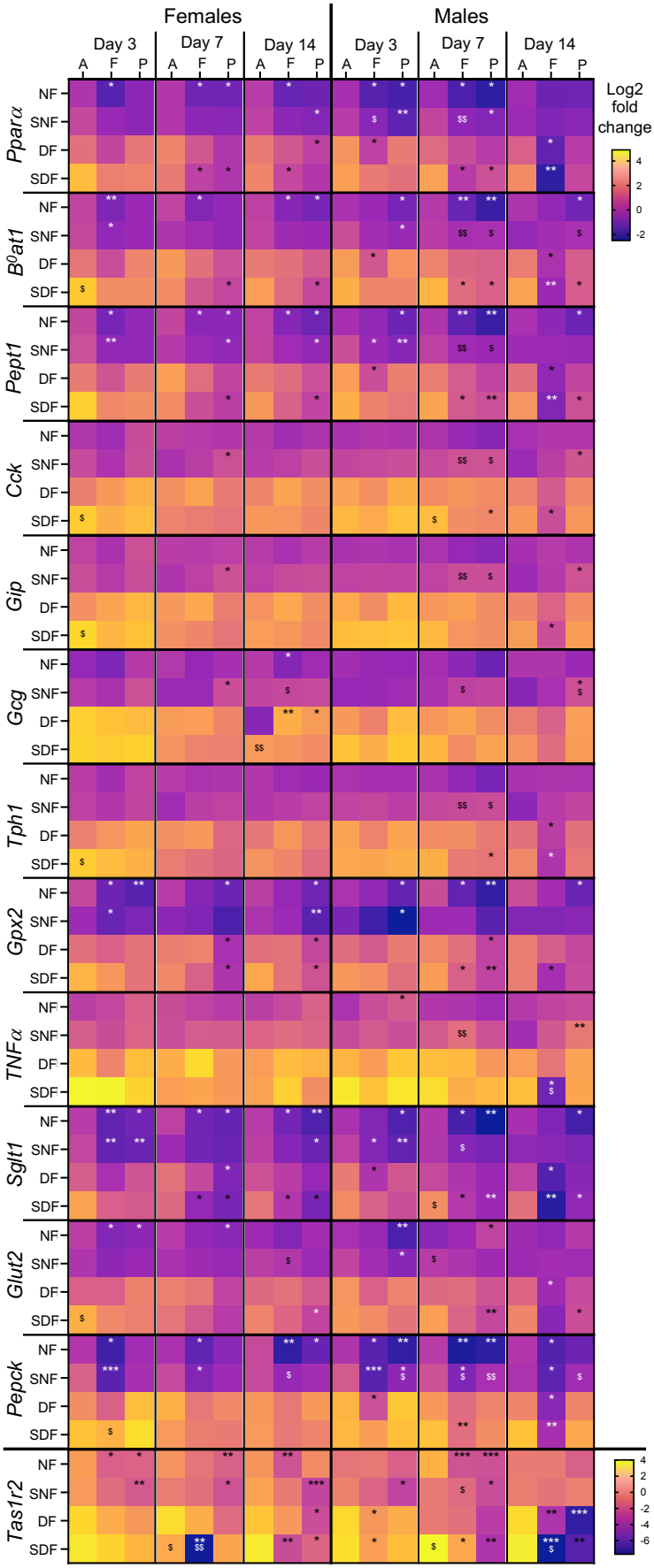

Figure 6. Diurnal and baseline gene expression changes in duodenum in response to TRF. Sample collection timepoints shown at the top: A = food anticipation, F = food intake, P = postprandial period. Feeding conditions shown on the left: NF = night-fed (ZT12 – ZT20), SNF = shifted night-fed (ZT16 – ZT24), DF = day-fed (ZT0 – ZT8), SDF = shifted day-fed (ZT4 – ZT12). Relative gene expression values (Log2) normalized to NF male mice on sacrifice day 3 at food anticipation and shown as means, n= 4-5 mice. Non-parametric Kruskal-Wallis test with Dunn's multiple comparison test used to show diurnal (vs. food anticipation) expression differences, *p<0.05, **p<0.01, ***p<0.001. The same test used to assess baseline differences (non-shifted vs. shifted) at each timepoint, $p<0.05, $$p<0.01.